ONLINE JOURNAL OF BIOLOGICAL SCIENCES

RESEARCH ARTICLE

Hydrophysical Properties of Soils as Indicators of the Hydrological Role of Rudny Altai Forests

Andrey Kalachev [1], Tamara Burenina [2], Stanislav Rogovsky [1], Elena Nikulina [1], Aida Kuldarbek [1], Victoria Rogovskaya [1], Elibek Assangaliev [3], Baitak Apshikur[3]*

[1]Altai branch of A.N. Bukeikhan Kazakh Research Institute of Forestry and Agroforestry, Ridder, Kazakhstan
[2]V.N. Sukachev Institute of Forest Siberian Branch of the Russian Academy of Sciences, Krasnoyarsk, Russian
[3]School of Earth Sciences, D. Serikbayev East Kazakhstan Technical University, Ust- Kamenogorsk, Kazakhstan

*Corresponding Author: bapshikur@edu.ektu.kz

Abstract: The hydrophysical properties of soils and parent rock are key factors shaping forest hydrological functioning, as they influence multiple runoff components. This study assessed the effects of forest stand composition on soil moisture and water permeability between 2021 and 2023 in the middle mountain-taiga zone of the Rudny Altai, within the Zhuravlikha River basin, a tributary of the Irtysh River. Measurements conducted at depths of 10-50 cm showed that Fir forests maintained the highest soil moisture across all layers. Although a 40-year-old birch stand had lower moisture content than Fir stands, it exhibited relatively high values in the upper soil horizon. Aspen stands demonstrated reduced moisture-retention capacity during the growing season due to high transpiration demand. Soil water permeability varied according to soil texture and vegetation type, with mean rates of 307±31.1 mm/h in birch stands, 409±62.33 mm/h in Aspen stands, 531±122.96 mm/h in Fir stands, and 648 ± 94.15 mm/h in shrublands. These findings highlight the role of forest composition in regulating soil hydrophysical properties essential for regional hydrological processes.

Keywords: Soil Moisture, Water Permeability, Forest Stands, Hydrological Role, Rudny Altai

Received: 25-02-2025 | **Revised:** 21-04-2025 | **Accepted:** 17-07-2025 | **DOI:** 10.3844/ojbsci.2026.26.01.003

Introduction

Forests play a key role in regulating hydrological processes, including interception, infiltration, evapotranspiration, and runoff redistribution. Their hydrological function is strongly controlled by soil physical properties, vegetation composition, and regional climate conditions [1-4].

Previous studies have investigated the partitioning of tree water use between transpiration and internal storage in mixed forest ecosystems. For example, Liu et al. reported that Platycladus orientalis and Quercus variabilis utilized soil water from different depths depending on season [5]. During the rainy season, *P. orientalis* relied primarily on surface soil layers (0-20 cm), while *Q. variabilis* maintained uptake from deeper horizons. Notably, 6-7% of annual sap flow in both species contributed to internal storage, demonstrating the importance of accounting for trunk-stored water in hydrological models.

Long-term monitoring remains essential for evaluating how land-use change influences soil moisture dynamics. Studies from the Loess Plateau have shown that artificial afforestation increases surface soil moisture (0-20 cm) through enhanced

litter accumulation, whereas deeper layers (20-100 cm) may gradually dry, reducing ecosystem productivity and long-term forest viability [6].

Soil hydrological constants-including minimal moisture capacity, capillary moisture, and wilting point-define the soil water retention potential under forest vegetation. Differences in granulometric composition cause strong contrasts between soil types: gray forest soils exhibit moisture capacity of 31-39%, while soddy-podzolic soils seldom reach 6% [7]. This demonstrates the broad variation of water-holding capacity driven by texture and genetic horizons [8].

Soil moisture exhibits pronounced seasonal dynamics determined by runoff formation and snowmelt processes. Dai and Cheng emphasized the importance of topsoil hydrodynamics in mountainous basins, while Apshikur et al. noted that soil moisture reserves reach near-capacity conditions twice per year (April and October), suggesting October as the effective onset of the hydrological year [9, 10].

Recent investigations have demonstrated that warming enhances summer soil moisture deficits. In Bryansk oblast, summer soil moisture in the active layer (to 1 m) declined between 1976 and 2010, increasing drought frequency [11-13]. At a longer time scale, δ^{13}C-cellulose records from Altai peat cores indicate a progressive moisture increase during the past 8000 years due to combined precipitation and temperature effects [14].

Advances in physically based modeling have deepened understanding of runoff generation and subsurface flow mechanisms [15]. Concurrently, data-analytic tools applied in smart-agriculture frameworks highlight the growing relevance of software-supported environmental assessment [16].

Topography, soil type, and climatic regimes regulate hydrological pathways across forest ecosystems [17-18]. In mountainous regions, aeolian and pedogenic processes strongly influence soil development, while in situ interventions can improve water retention capacity [19, 20]. Plant community composition also affects hydrological functioning through control of soil properties and nutrient cycling [21]. Forest diversity contributes to the long-term accumulation of soil organic carbon and nitrogen, supporting hydrological stability [22].

Siberian Fir (Abies sibirica Ledeb.) dominates the dark-coniferous mountain forests of the Rudny Altai, accompanied by birch (Betula pendula) and Aspen (Populus tremula). These forests provide soil protection, water conservation, and air-quality regulation. However, wildFire and logging during the past two centuries have altered stand composition, affecting water-protective and water-regulating functions [23]. Thus, assessment of soil hydrophysical properties is essential for understanding hydrological regulation in degraded and secondary forests.

This study investigates soil moisture and water permeability in mature and secondary forest ecosystems of the Rudny Altai. These parameters are key indicators of water-regulation and soil-protection capacity, reflecting vegetation type, soil structure, and mechanical composition.

We hypothesize that forest stand composition and structure significantly influence soil hydrophysical properties, including moisture retention and permeability.

The objective of this study is to evaluate the hydrological role of forest stands with different structural and inventory characteristics by measuring soil moisture and water permeability across contrasting phytocenoses.

Materials and Methods

The study of hydrophysical soil properties was carried out at monitoring sites located within the middle mountain-taiga belt of the Rudny Altai, on west-facing slopes with gradients of 15-25°. The sites lie within the Zhuravlikha River basin, a tributary of the Ulba River, forming part of the Upper Irtysh runoff-formation area. The monitoring plots, situated at elevations of 930-970 m above sea level are characterized by dominant coniferous and mixed forest stands and relatively undisturbed environments, ensuring uniform climatic conditions across the study area.

These areas are ecologically significant due to their role in regulating hydrological processes and runoff formation. In addition, the plots are located in regions with a long history of forestry and hydrological observations, enabling comparison with previously collected regional data. The geographic location of the plots is presented in Figure 1, and the main forest-inventory characteristics are summarized in Table 1.

DOI: 10.3844/ojbsci.2026.26.01.008

The hydrophysical properties of the soil cover at the studied sites were assessed using generally accepted methodologies. To characterize the mechanical and chemical properties of the soils, full soil profiles were excavated at each monitoring plot, and samples were collected from corresponding genetic horizons for subsequent laboratory analysis.

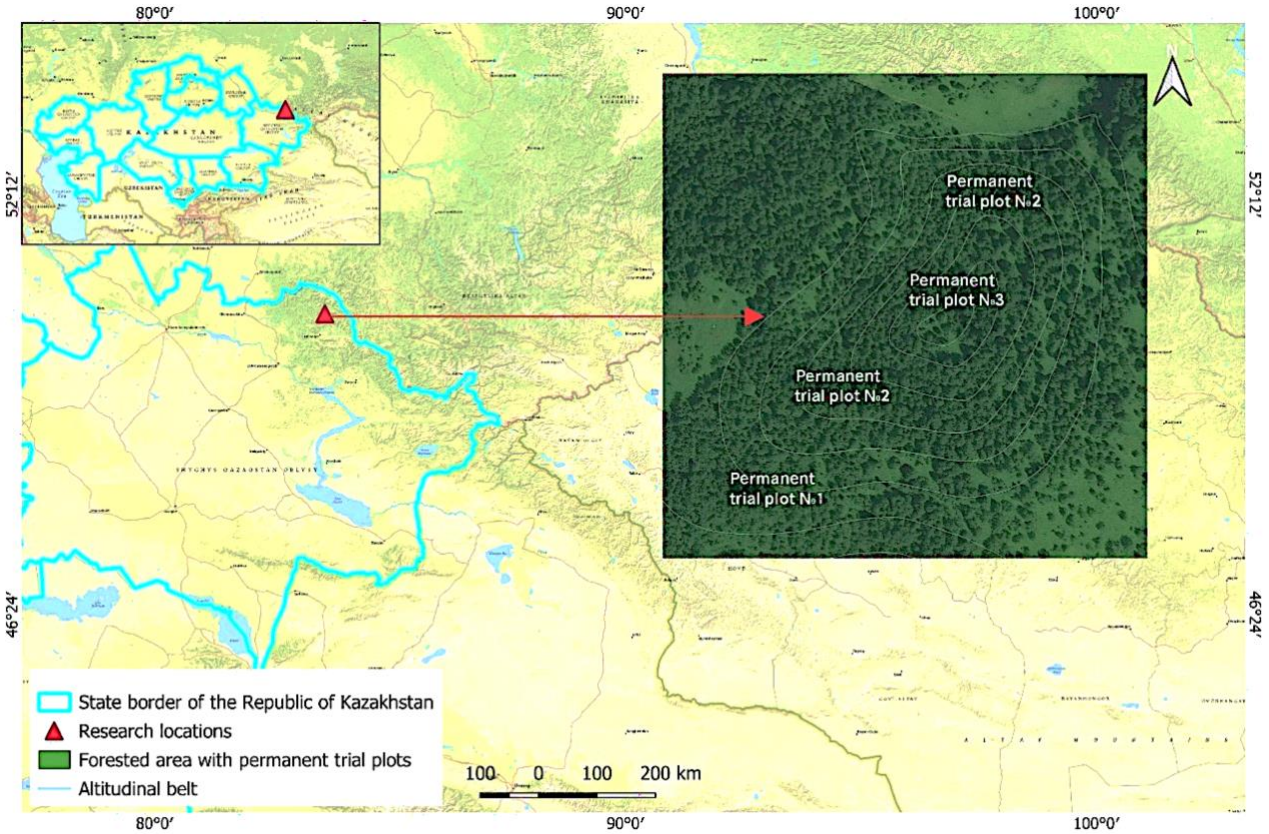

Fig. 1: Geographical location and spatial distribution of permanent trial plots in the Rudny Altai region

Table 1: Forest inventory indicators of monitoring sites

No.	Composition	Phytocenoses	Age (Years)	Height (m)	Diameter (cm)	Class Quality	Stock (m^3/ha)	Density of Stands	Total area (ha)
1	10B	Birch forest stand with grass	41	15.6	14.9	I	180 ± 9	1.09 ± 0.05	1.09
2	10As+B	Aspen forest stand with grass and ferns	*As 60	22.0	22.0	I	229 ±11	0.81 ± 0.04	0.81
			*B 59	21.6	27.3				
3	8F2B	Fir forest stand with grass and ferns	*F 80	17.3	20.7	III	135 ±10	0.72 ± 0.03	0.72
			*B 80	18.0	36.8				
4	8 Azh 2Tv	Shrubbery	*Azh	1.5	2.0	V	-	-	0.5
			*Tv	1.5	1.0				

*F - Fir, B - birch, As - Aspen, Azh - yellow acacia, Tv - meadowsweet (medium spirea)

To measure soil moisture, the thermostatic-weight method was employed [24] (Brevik et al., 2021), which was used to determine the natural gravimetric moisture content (W).

Although the thermostatic-weight method served as the primary technique [25] (Li et al., 2023), results were additionally cross-validated using standard gravimetric analysis to improve accuracy and consistency. For this purpose, selected samples were oven-dried at 105 °C for 24 hours and the obtained values were compared with those from the thermostatic method.

Soil samples to determine its moisture content were taken on a monthly basis at sample plots. Sampling for the study of natural moisture in the test plots was carried out with a soil drill. Samples were taken in 3 replicates. Mass or weight natural moisture content Eq. 1 calculated (W).

$$w\%\ by\ mass = \frac{b-c}{c-a} * 100\% \quad (1)$$

Where:

a- is the weight of the bottle, (g);

b- is the weight of the weighing bottle with wet soil, (g);

c - weight of bottle with absolutely dry soil, (g);

(b - c) is the mass of water, (g);

(c - a) is the mass of dry soil, (g).

Soil sampling depths were selected according to commonly recognized soil horizon boundaries and the observed root distribution within each phytocenosis. Standard depth intervals (e.g., 0-10 cm, 10-20 cm, 20-30 cm, etc.) were maintained across all sites to ensure consistency and comparability. Minor adjustments to sampling depth were made only when shallow bedrock or dense gravel layers were encountered.

The Kachinsky tube method was used to determine soil water permeability [4, 26]. For field measurements, metal cylinders with an internal diameter of 5 cm and a height of 13 cm were employed. Each tube was inserted 3 cm into the soil, and the initial water column height was set to 10 cm. The lower edge of the tube was sharpened to facilitate insertion. A total of ten tubes were installed at each site, positioned 13-15 cm apart in two staggered rows. Because soil water permeability strongly depends on soil moisture content, moisture levels were measured concurrently using the thermostatic-weight method [24].

After the tubes were installed, water was introduced into each cylinder using a siphon device. Observations were conducted for a minimum of three hours. Based on the measurements obtained, the moisture flux *q* (cm/min) was calculated using Equation 2, where *q* represents the volume of water *Q* (cm³) that infiltrated into the soil per unit time *t* (min) through the unit cross-sectional area *S* (cm²) of the cylinder.

$$q_w = \frac{Q}{S \cdot t} \quad (2)$$

To ensure measurement reliability, soil permeability was assessed using 10 replicates at each site. The resulting data were statistically processed to obtain mean values and standard deviations; summary statistics are presented in the *Soil Permeability* section. This approach helped account for natural variability in soil structure and moisture distribution across micro-sites [27].

To ensure comparability of measurements obtained under different water temperatures, all permeability values were standardized to a reference temperature of 10 °C using Hazen's correction coefficient (0.7 + 0.03 T °C) Eq. 3.

All measurements were performed in triplicate, and results are presented as mean ± standard deviation. Descriptive statistical analyses were conducted to characterize variability among sites; these differences are discussed in the Results section. Additional statistical comparisons (e.g., ANOVA, correlation analyses) are planned for future studies as the dataset is expanded.

$$K_{10} = \frac{K_f}{0{,}7 + 0{,}03\ \mathrm{T}\ ^\circ\mathrm{C}} \quad (3)$$

Where:

K_f -is the filtration coefficient at a given temperature;

T °C -is the water temperature in the observation interval;

0.7 and 0.03 -are empirical coefficients.

Water temperature corrections were uniformly applied across all observation sites using Hazen's empirical equation, allowing standardization of permeability values to a reference temperature of 10 °C. This ensured consistency among measurements and minimized temperature-related bias.

For uniformity, soil permeability results are reported in millimeters per hour (mm/h), while soil moisture content is expressed as a percentage of dry soil mass. Terminology, including the term hydrophysical properties, is used consistently throughout the manuscript [4].

To classify the degree of soil water permeability, N.A. Kachinsky's permeability scale was applied Table 2.

Table 2: Water permeability scale by N. A. Kachinsky

Perforating water permeability (extremely high)	More than 1000 mm/hour (at 10º C)
Excessively High	1000-500 mm/hour
The Best	500-100 mm/hour
Good	100-70 mm/hour
Satisfactory	70-30 mm/hour
Unsatisfactory	less than 30 mm/hour

Results and Discussion

Soil profiles were established within each forest type to characterize the mechanical and chemical properties of the soils in the monitoring areas. The particle-size distribution of soil samples collected at different depths is presented in Table 3. The table summarizes the proportion of sand, silt, and clay fractions (expressed as percentage of dry soil), the combined content of particles <0.01 mm and > 0.01 mm, as well as hygroscopic moisture. These parameters provide insight into the physical structure of the soils and their potential to retain water and support hydrological processes in different forest stands.

Table 3: Mechanical composition of soils

Forest type	Sample depth cm	The number of fractions as a percentage of dry soil								Hygroscopic moisture, %
		1 - 0.25	0.25-0.05	0.05-0.01	0.01-0.005	0.005-0.001	0.001	Sum of fractions		
								<0.01	>0.01	
Birch forest stand with grass	0-5	0.16	30.24	33.47	12.97	11.67	11.50	36.14	63.86	7.14
	5-20	0.15	44.86	21.30	11.74	10.55	11.40	33.69	66.31	6.31
	20-40	0.11	35.37	21.92	16.10	12.74	13.75	42.59	57.41	4.58
	40-70	0.11	28.84	30.24	13.99	11.93	14.89	40.81	59.19	2.78
	70-76	0.15	30.73	27.96	14.06	14.02	13.09	41.16	58.84	1.27
Aspen forest stand with grass and ferns	0-10	0.96	44.82	21.44	11.39	10.31	11.09	32.79	67.21	7.65
	10-24	1.04	42.00	22.54	11.73	12.85	9.85	34.43	65.57	3.80
	24-30	0.66	41.66	23.35	10.57	14.80	8.96	34.33	65.67	2.71
Fir forest stand with grass and ferns	0-14	0.14	18.16	16.38	39.86	10.75	14.72	65.33	34.67	13.30
	14-35	0.13	31.62	24.60	19.79	9.62	14.23	43.64	56.36	4.41
	35-62	0.15	29.20	23.63	20.74	10.78	15.49	47.02	52.98	3.18
	62-70	0.18	32.88	24.44	17.48	11.05	13.96	42.50	57.50	1.17
Shrubbery	0-10	0.17	18.97	16.00	41.91	13.39	9.55	64.86	35.14	12.49
	10-20	0.21	25.72	23.38	37.80	13.91	8.98	60.68	39.32	8.25
	20-30	0.98	31.79	27.81	14.28	15.35	9.85	39.48	60.52	3.35
	30-35	0.58	29.04	30.63	13.68	15.68	10.40	39.76	60.24	2.31

Birch Forest Stand

The birch forest stand (composition: 10B) is located in the central part of the study area. The forest type corresponds to birch stands with grass (Bgr). The undergrowth is sparse and is represented by Spiraea media L., Caragana arborescens Lam., and Ribes rubrum L.

The herbaceous layer is dense and dominated by tall grasses and forbs, including Veratrum lobelianum Bernh., Crepis sibirica L., Aconitum septentrionale Koelle, Angelica archangelica L., Angelica silvestris L., Heracleum dissectum Ledeb., Bupleurum aureum (Fisch. ex Hoffm.), Lathyrus gmelinii Fritsch, and Paeonia anomala L.

The regeneration layer is poorly developed, consisting mainly of scattered young Fir (5-12 years) and occasional birch. This phytocenosis represents a secondary forest stand.

A0 (0-5 cm). Loose sod layer, densely penetrated by roots with abundant plant residues.

A1 (5-20 cm). Gray-colored horizon, strongly penetrated by woody and herbaceous roots; structure is loose and crumbly to granular; transition is clear.

A2 (20-40 cm). Light gray, permeated with fine roots; light loam in texture; fine nutty structure; transition to the next horizon is distinct.

B (40-70 cm). Brown with a grayish tint; nutty-blocky structure; moist, compacted heavy loam with gravel inclusions; gradual transition.

BC (70-86 cm). Light brown, moist, medium loam; blocky structure with abundant crushed stone.

C (> 86 cm). Clay-rich parent material.

Soil type: mountain forest gray.

Aspen Forest Stand

The plot is located in the middle part of the study area. The stand composition is 10As, and the forest type is an Aspen forest with grass and ferns.

The undergrowth is dense and heterogeneous, represented mainly by Caragana arborescens (yellow acacia) and Ribes rubrum (red currant).

The herb layer is dominated by tall forb species (20 cm-1.0 m), including Acónitum septentrionále (tall monkshood), Delphinium elatum L. (high larkspur), ferns (Dryópteris fílix-mas L., Athýrium fílix-fémina L.), Artemísia absínthium L. (wormwood), Hypericum perforatum L. (St. John's wort), Bupleúrum auréum (golden bupleurum), Crepis sibirica L. (Siberian skerda), Veratrum lobelianum (Lobel's hellebore), Thalictrum aquilegiifolium L. (meadow-rue), Paeónia anómala L. (evasive peony), and others.

Among the grasses, dominant species include Dactylis glomerata L. (orchard grass), Milium effusum L. (wood millet), Bromus inermis Leyss. (smooth brome), and sedges (Carex altaica (Gorodkov) V.I. Krecz.; C. sylvatica).

In the regeneration layer, Abies sibirica (Fir) occurs only sporadically, with individual trees exceeding 20 years of age. The stand is of secondary origin.

A_0 (0-10 cm). Dark gray, loose sod layer, strongly penetrated by roots; contains abundant plant residues.

B (10-24 cm). Light brown horizon, densely penetrated by woody and herbaceous roots; sandy-loam material with scattered stones; clear boundary.

BC (24-40 cm). Light brown with a grayish tint; nutty-lumpy structure; moist, heavy loam; compacted with a substantial amount of crushed stone.

C (> 40 cm). Clay and parent rock.

Soil type: mountain forest gray.

Fir Forest Stand

This monitoring plot is located in the central part of the study area.

The stand belongs to age class IV and has a composition of 8F2B. The average tree height and diameter are 17.3 m and 20.7 cm, respectively. The total basal area is 16.57 m²/ha, with a relative density of 0.72. The quality class is III, and the total growing stock is 170 m³/ha, including 135 m³/ha of Fir and 35 m³/ha of birch. The forest type is a Fir stand with grasses and ferns.

Undergrowth is dominated by Siberian Fir (0.3-2.0 m in height), with occasional birch and Aspen. The shrub layer is dense and consists of mountain ash (Sorbus sibirica Hedl.), raspberry (Rubus idaeus L.), elderberry (Sambucus racemosa L.), bird cherry (Padus L.), yellow acacia, and currant, distributed evenly across the site.

The main grass species include awnless brome, blunt reed grass (Calamagrostis agrostioides Matuszk), giant fescue (Festuca gigantea L.), and drooping barley grass (Melica nutans L.). Forbs (5-40 cm in height, up to 1.0 m along edges) beneath the canopy are represented by Oxalis acetosella L., fragrant woodruff (Asperula graveolens Bieb), forget-me-not (Myosotis L.), two-flowered violet (Viola biflora L.), bedstraw, columbine, crow's-eye (Paris quadrifolia L.), and mosses (Bryophyta).

In clearings, forest margins, and open areas, the vegetation includes peony (Paeonia anomala L.), ferns, Lobel's hellebore, bitter saussurea (Saussurea amara L.), field watercress (Cirsium arvense L.), blue cyanosis (Polemonium caeruleum L.), forest woundwort (Stachys sylvatica L.), goldenrod (Solidago virgaurea L.), hogweed, and others.

A notable feature of the site is the presence of dead wood.

A1 (0-14 cm). Loose loamy turf, densely penetrated by fine roots, with abundant plant residues.

A2 (14-35 cm). Gray with a light-brown tint, strongly penetrated by woody and herbaceous roots; light loam, moist, with a lumpy structure and loose texture; clear transition to the next horizon.

B (35-62 cm). Brown with a grayish tinge, nutty-lumpy structure, moist, heavy loam, compacted; gradual transition.

BC (62-70 cm). Brown, moist, medium loam, lumpy structure, dense, with a significant amount of crushed stone.

C (>70 cm). Clay and parent rock.

Soil type: mountain forest gray.

Shrubbery (Bush Thickets)

The soil profile was established in the upper part of the sample plot, where dense thickets of yellow acacia dominate, with spirea also present. The shrubs reach approximately 1.5 m in height and 2.0 cm in diameter. The closure of the shrub-herb layer within the plot is 90-95%.

In the open southwestern-exposed areas of the site, outcrops of parent rock with shallow soils and herbaceous vegetation are observed. Grasses and sedges predominate. Common herbaceous species include Galium L., oregano (Origanum vulgare L.), columbine (Aquilegia vulgaris L.), and bladder campion (Silene vulgaris (Moench) Garcke).

A1 (0-10 cm) — Loose gray turf, strongly permeated with fine roots and containing abundant plant remains; interspersed with fine gravel.

A2 (10-20 cm). Loose gray material, heavily penetrated by shrub and herb roots; light loam, moist, with a lumpy structure and loose texture; contains crushed stone of small, medium, and large fractions.

B (20-30 cm). Brown with a grayish tint; heavy loam, compact, with a gradual transition; interspersed with medium and large fragments of crushed stone.

BC (30-35 cm). Compact sandy loam; parent rock influence evident.

C (>35 cm). Parent rock.

Soil type: mountain forest gray.

DOI: 10.3844/ojbsci.2026.26.01.008

Soil moisture

Soil moisture is a key parameter for numerous scientific and practical applications, including the assessment of water-balance components across various spatial and temporal scales [28, 29] (Shehata et al., 2022; Abdi et al., 2020). Precipitation is considered the primary factor influencing soil moisture and evapotranspiration [30] (Condon et al., 2020).

Analysis of the obtained data revealed a general trend of decreasing soil moisture with increasing sampling depth. At all sites, moisture content declined consistently from the upper layers to deeper horizons, as illustrated in Figure 2.

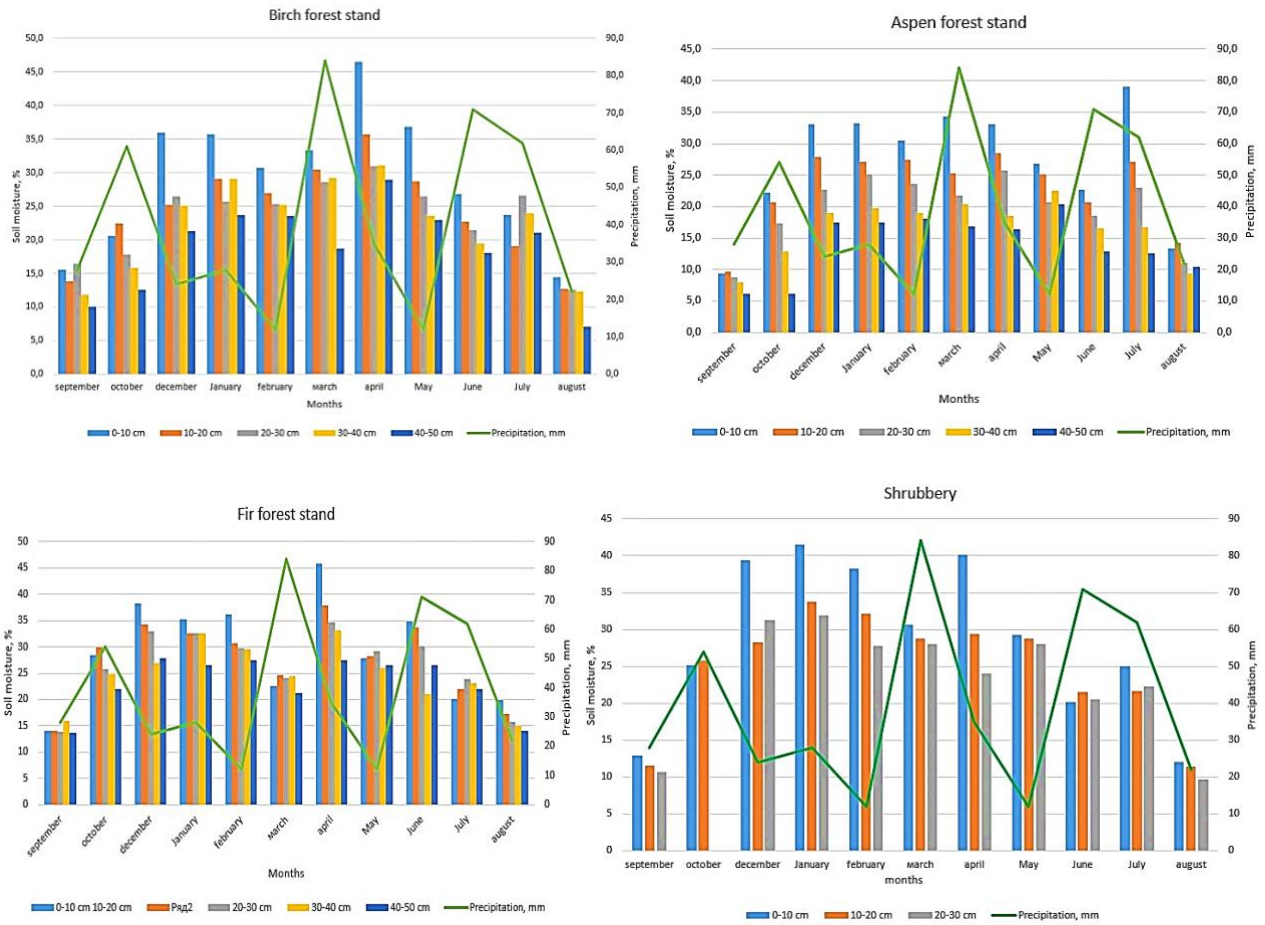

Fig. 2: Change in soil moisture indicators at monitoring sites for the period September 2021 - August 2022

This pattern may be explained by the fact that, due to the high gravel content of the soils, groundwater occurs at considerable depths and therefore does not influence the upper soil horizons. In contrast, the forest litter and humus horizons are capable of accumulating and retaining moisture for extended periods.

Notable differences in moisture variation within the same horizons were observed among different phytocenoses. The upper soil layers in the birch stand exhibited higher moisture content compared with those in the Fir and Aspen forests. Among all examined phytocenoses, the Fir stand showed the highest overall soil moisture, with a more uniform vertical distribution than that found in deciduous stands or shrublands. Elevated moisture levels in Fir stands persisted even at the maximum sampling depth, as clearly illustrated in the graph.

Although the upper horizon of the Fir stand stored less moisture than that of the birch stand, the soil cover under Fir remained relatively stable in terms of moisture content down to a depth of 50 cm.

The lowest soil moisture observed in the Aspen stand is likely associated with its higher transpiration demand. According to published findings, transpiration intensity in Aspen within taiga ecosystems is 1.5 times greater than that of birch and 2-3

times greater than that of Fir. Mänttäri et al. also reported that moisture consumption for transpiration in 50-year-old Aspen stands is approximately 40% higher than in Fir stands of comparable age [31].

Seasonal variability in soil moisture was clearly observed across all phytocenoses. The moisture reserves increased significantly in early spring (April) due to snowmelt, while declining sharply in summer months, particularly during periods of abnormal weather such as May 2022, which saw elevated temperatures and minimal precipitation. These fluctuations reflect the strong sensitivity of soil moisture to extreme climate events, including drought periods and rapid warming trends.

These seasonal dynamics are consistent with observations from high-elevation forest ecosystems of the Polar Urals, where long-term warming has intensified stand productivity and resulted in an upward shift of the upper treeline, consequently altering soil-water conditions [32].

The highest soil moisture values across all study sites occurred in April, during peak snowmelt. In winter, elevated soil moisture is maintained due to substantial snow accumulation and reduced plant water uptake. Periodic thaws additionally influence moisture content in the upper horizons.

Patterns of moisture change with depth differ among phytocenoses during the cold season. In the Aspen stand, moisture declined sharply below 30 cm, reaching 17-18%. In contrast, in the Fir stand, moisture remained consistently high (25-30%) throughout the profile. These differences can be explained by variation in soil texture: in the Fir stand, light-textured fractions constitute up to 65% of total mass, while in birch and Aspen soils they account for less than 35% (Table 3).

In March, the Fir stand showed minimum moisture values across all horizons, unlike other ecosystems. Higher moisture content in birch and Aspen upper horizons results from earlier snowmelt and subsequent infiltration, whereas snowmelt is absent under Fir at this time.

Except in Aspen stands, maximum soil moisture across all profiles occurred in April, corresponding to peak snowmelt and above-normal precipitation. March 2022 precipitation exceeded long-term averages by 2.5 times; snow water equivalents reached 321 mm in Aspen stands and 408 mm in Fir stands. Rapid warming in April-May (+1.8 °C anomaly) contributed to intense snowmelt and deep wetting of soils.

By May, soil moisture in all ecosystems decreased across all horizons (except 0-10 cm in birch). Mean air temperature was 15.2 °C (4.1 °C above normal), and total precipitation was only 12 mm (17% of normal), resulting in strong evapotranspiration and depletion of soil moisture to depths of at least 50 cm. The higher moisture in the upper horizon of the birch stand was likely due to lower transpiration demand and the moderating influence of accumulated litter.

In June, soil moisture continued to decline in all stands except Fir, due to high transpiration rates in deciduous stands and insufficient recharge following the dry May. Despite near-normal precipitation in June (71 mm), July moisture remained low; high temperatures (mean 17.1 °C, max 30.1 °C) sustained elevated evaporative losses. Fir stands maintained the highest soil moisture across all horizons (10-50 cm). Overall, the 40-year-old birch stand stored less moisture than Fir, although its upper horizon remained relatively moist. Aspen stands were the least effective at conserving moisture during the growing season due to high transpiration demand.

Comparisons with other regions support these findings. In the dark coniferous taiga of the Western Sayan, soil moisture in Aspen and Aspen-Fir stands were nearly twice as high [33], likely due to higher precipitation, cooler summers, and lower transpiration. Similarly, mixed temperate forests of Central Europe exhibit lower permeability associated with heavier soil textures and higher organic matter accumulation. These contrasts emphasize the strong influence of regional climatic and edaphic conditions on forest-soil hydrology.

The reduced water retention capacity at greater depths (>50 cm) is attributed to parent material dominated by gravel and stony fragments. This is especially pronounced in shrub and Aspen stands. Future studies should extend sampling to deeper horizons (>70 cm) to better evaluate subsoil contributions to moisture storage and groundwater recharge.

Soil Permeability

Soil infiltration characteristics are key indicators of the hydrological functioning of forest phytocenoses. Water permeability, defined as the ability of soil to transmit water, reflects the rate of gravitational water infiltration. Numerous forest-hydrology studies have shown that water-regulating and protective functions of forest stands are closely linked to soil permeability. When

DOI: 10.3844/ojbsci.2026.26.01.008

permeability is low, a portion of atmospheric precipitation flows across the surface, promoting soil erosion. Soil permeability is highly variable and largely depends on soil moisture content.

Soil water permeability was quantified using the Kachinsky tube method, which measures infiltration rates through metal cylinders installed at defined soil horizons. The installation procedure is shown in Figure 3. Soil permeability and corresponding moisture content for each experimental plot at the time of sampling are presented in Table 4.

Mean infiltration rates (mm/hour) derived from three replicates (n = 3) per depth layer are shown in Figure 4. Measurements were obtained at standard depths of 0-10 cm, 11-20 cm, and 21-30 cm, and represent typical hydrological conditions for the examined forest types and shrublands.

Fig. 3: Installation of Kachinsky infiltration tubes for soil water-permeability measurements

Table 4: Indicators of soil water permeability on test plots

No. Plot	Vegetation characteristics	Soil depth (cm)	Soil moisture at the time of the experiment	Soil Water Permeability, K_{10}, mm/hour	Water Permeability
1	Birch forest stand with grass	0-10	34 %	372	the best
		10-20	16 %	310	the best
		20-30	21 %	240	the best
2	Aspen forest stand with grass and ferns	0-10	22 %	546	excessively high
		10-20	12 %	401	excessively high
		20-30	15 %	282	the best
3	Fir forest stand with grass and ferns	0-10	23 %	832	excessively high
		10-20	25 %	371	the best
		20-30	15 %	390	the best
4	Shrubs (yellow acacia, medium spirea)	0-10	18.2 %	876	excessively high
		10-20	13.0 %	504	excessively high
		20-30	17.9 %	564	excessively high

DOI: 10.3844/ojbsci.2026.26.01.008

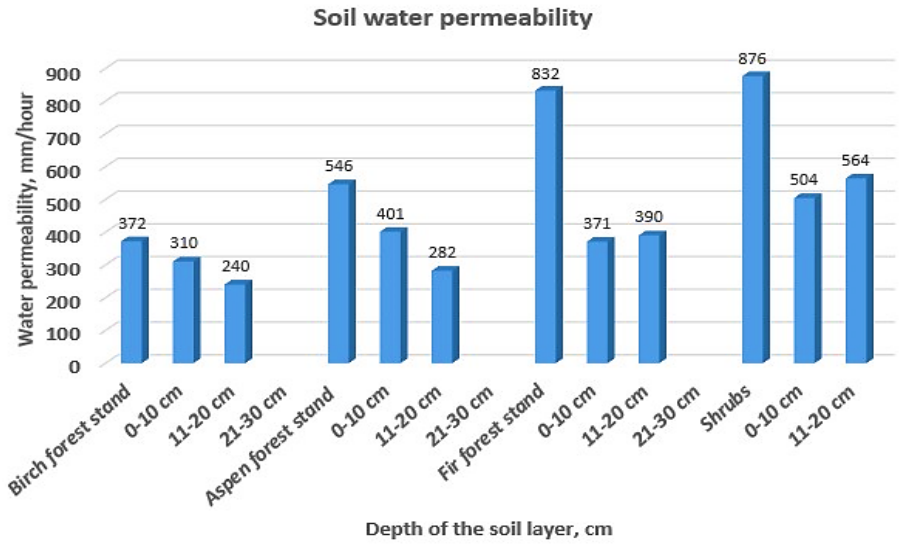

Fig. 4: Average water permeability of soils at different depths across vegetation types

Analysis of the data shows that soil water permeability increases from deciduous stands to coniferous stands and shrublands. Mean values were 307 ± 31.1 (mm/hour) in the birch stand, 409 ± 62.33 (mm/hour) in the Aspen stand, 531 ± 122.96 (mm/hour) in the Fir stand, and 648 ± 94.15 (mm/hour) in the shrubland.

Given that all study sites are located under comparable climatic conditions, these differences are believed to result primarily from variation in mechanical soil composition (Table 3) and vegetation structure.

As noted above, the birch stand showed the highest moisture content in the upper soil horizons, which coincided with the lowest water permeability. In contrast, Aspen and Fir stands exhibited lower moisture content in the upper horizons and, correspondingly, higher permeability. The shrubland had the lowest soil moisture and the highest permeability values.

Soil permeability in the Fir stand was more than twice that in the birch stand and 1.5 times higher than that in the Aspen stand. This underscores the role of forest litter in absorbing atmospheric precipitation [34] and converting surface runoff into subsurface flow. The hydrological function of the litter layer is particularly important in coniferous forests, where its accumulation ranges from 40 to 100 (t/ha) depending on stand composition, age, and density [35].

The very high permeability observed across all horizons in the shrubland is likely associated with the shallow depth and coarse texture of the soil profile. Fine to medium gravel is present from 15-30 cm, transitioning to fragmented bedrock at - 30 cm depth. Low soil moisture may also reflect high evapotranspiration losses.

Comparison with published data from Fir forests of the Yenisei Ridge [28] and boreal forested watersheds of British Columbia, Canada [36] indicates that, despite similar forest cover, soil permeability within the Zhuravlikha River basin is nearly 50% lower than in mountainous regions of southern Siberia. This difference likely reflects regional variation in soil structure, climatic conditions, and disturbance history.

On the Yenisei Ridge, soils may contain up to 70-80% gravel, producing a leaching-type water regime. Extremely high permeability in Fir stands there is associated with mountain soddy-forest soils underlain by shale and gneiss. These soils are thin, granular-cloddy or platy, and well drained by dense tree and shrub root systems.

In contrast, the soils on the monitored slopes of the Rudny Altai are moderately deep, lightly loamy, contain significant gravel, and show weak horizon differentiation, which collectively promotes relatively high permeability. Vegetation further modifies infiltration patterns in the upper horizons. The greatest infiltration capacity occurred in the upper layers of the Fir forest and shrubland.

Conclusion

The results of this study demonstrate that forest type exerts a strong influence on the hydrophysical properties of soils in the Rudny Altai region. Fir stands exhibited the highest soil moisture content across all investigated horizons (10-50 cm), whereas birch stands were characterized by high moisture retention mainly in the upper soil layers. Aspen stands showed markedly lower moisture content, particularly during the growing season, likely due to elevated transpiration rates.

Soil water permeability also varied considerably among phytocenoses, increasing from deciduous to coniferous stands and reaching maximum values in shrublands. Shrub thickets exhibited the highest infiltration capacity (648 ± 94.15 mm/hour), while birch forests demonstrated the lowest rates (307 ± 31.1 mm/hour). These findings highlight the regulatory influence of vegetation type, forest litter accumulation, and soil structural characteristics on infiltration and water retention processes.

From an applied standpoint, the preservation or restoration of coniferous stands in erosion-prone or snow-accumulation zones could enhance subsurface infiltration and reduce surface runoff, thereby promoting more stable watershed hydrology. Conversely, shrub-dominated communities with high permeability may be suitable for areas where rapid drainage is required.

Overall, the study underscores the importance of considering the interactions among vegetation, soil structure, and hydrological dynamics when designing forest and watershed management strategies. Such measures may support long-term ecosystem resilience under increasing climatic variability and contribute to the sustainable use of regional water resources.

Acknowledgment

The authors express their gratitude to the Altai branch of the Kazakh Research Institute of Forestry and Agroforest Melioration named after A. N. Bukeykhan for providing research infrastructure, field support, and laboratory facilities that enabled the completion of this study.

Funding Information

This study was carried out within the framework of a scientific and (or) scientific-technical project funded by the Ministry of Ecology, Geology and Natural Resources of the Republic of Kazakhstan (IRN BR10263776) and implemented by the Altai branch of the Kazakh Research Institute of Forestry and Agroforest Melioration named after A.N. Bukeykhan.

Authors Contributions

Andrey Kalachev: Conceptualization, supervision, methodology development, final revision.

Tamara Burenina: Field investigation, sample collection.

Stanislav Rogovsky: Drafting the manuscript, critical revision.

Elena Nikulina: Laboratory analysis, manuscript revision.

Aida Kuldarbek: Laboratory experiments, manuscript preparation.

Victoria Rogovskaya: Data processing, manuscript revision.

Elibek Assangaliev: Data analysis, validation, theoretical development.

Baitak Apshikur: Project administration, correspondence, manuscript revision.

Ethics

This article is original and has not been published elsewhere. All authors have read and approved the final version of the manuscript. The study does not involve any ethical concerns, and no human or animal subjects were used in this research.

Conflict of Interest

The authors declare that they have no conflicts of interest.

References

1. Fan, Y., Miguez-Macho, G., Jobbágy, E.G., Jackson, R.B. and Otero-Casal, C. 2022. Hydrologic regulation by vegetation and groundwater in mountain forests. *Nature Reviews Earth and Environment*, 3(7): 515-531. DOI:10.1038/s43017-022-00269-w.
2. Zhang, L., Wang, J., Song, X. and Zhang, B. 2021. Hydrological responses to forest change in mountain watersheds: A meta-analysis. *Journal of Hydrology*, 603: 126905. DOI:10.1016/j.jhydrol.2021.126905.
3. Klaus, J., Zehe, E., Elsner, M., Külls, C. and Schroeder, B. 2021. Soil moisture dynamics and permeability across forest types. *Ecohydrology*, 14(1): e2251. DOI:10.1002/eco.2251.
4. Kalachev, A., Burenina, T., Rogovskiy, S., Nikulina, E., Rogovskaya, V. and Kuldarbek, A. 2023. Effect of forest stands of Rudny Altai (Eastern Kazakhstan) on snow cover formation. *Polish Journal of Environmental Studies*, 32(6): 5619-5630. DOI:10.15244/pjoes/169403.
5. Liu, Z., Liu, Q., Wei, Z. et al. 2021. Partitioning tree water usage into storage and transpiration in a mixed forest. *Forest Ecosystems*, 8: 72. DOI:10.1186/s40663-021-00353-5.
6. Mao, L., Miao, Y., Ge, Y. et al. 2024. Effects of different afforestation years on soil moisture and nutrient content. *Scientific Reports*, 14: 16194. DOI:10.1038/s41598-024-66408-z.
7. Lebedeva, T., Sokolov, D., Semenov, M., Zinyakova, N., Udaltsov, S. and Semenov, V. 2024. Organic carbon distribution between structural and process pools in gray forest soil. Dokuchaev Soil Bulletin, 118: 79-127. DOI:10.19047/0136-1694-2024-118-79-127.
8. Kayugina, S.M. and Eremin, D.I. 2022. Physicochemical properties of gray forest soils on the eastern outskirts of the Trans-Ural Plateau. *Journal of Siberian Federal University. Biology*, 15(4): 471-490. DOI:10.17516/1997-1389-0399.
9. Dai, J.Y. and Cheng, S.T. 2022. Modeling shallow soil moisture dynamics in mountainous landslide active regions. *Frontiers in Environmental Science*, 10: 913059. DOI:10.3389/fenvs.2022.913059.
10. Apshikur, B., Kurmangaliyev, T.B., Goltsev, A.G., Alimkulov, M.M. and Kapasov, A.K. 2023. The method of multi-criteria analysis for determining the flood-hazardous area and the development of protective structures. *ISPRS Archives*, XLVIII-5/W2-2023: 9-17. DOI:10.5194/isprs-archives-XLVIII-5-W2-2023-9-2023.
11. Shogelova, N., Sartin, S. and Zveryachenko, T. 2022. Devising recommendations based on a comprehensive assessment of the soil-geobotanical condition of land plots for executing afforestation activities. *Eastern-European Journal of Enterprise Technologies*, 2: 30-41. DOI:10.15587/1729-4061.2022.255054.
12. Roba, Z.R., Moisa, M.B., Purohit, S., Deribew, K.T. and Gemeda, D.O. 2025. Assessing the impacts of forest cover change on carbon stock and soil moisture dynamics. *Environmental Monitoring and Assessment*, 197: 169. DOI:10.1007/s10661-024-13611-0.
13. Apshikur, B., Alimkulov, M.A., Kapasov, A.K. and Toleubekyzy, I.T. 2024(a). Innovative technology for assessing the degradation of the Earth by sand desertification of soils with specialized processing of space materials. *InterCarto. InterGIS*, 30(2): 223-235. DOI:10.35595/2414-9179-2024-2-30-223-235.
14. Zhang, D., Feng, Z., Yang, Y.P., Lan, B., Ran, M. and Mu, G.J. 2018. Peat δ13C-cellulose-recorded wetting trend in southern Altai Mountains. *Journal of Asian Earth Sciences*, 156: 174-179. DOI:10.1016/j.jseaes.2018.01.029.
15. Lapides, D.A., Sytsma, A. and Thompson, S. 2021. Implications of distinct methodological interpretations and runoff coefficient usage for rational method predictions. *Journal of the American Water Resources Association*, 57(6): 859-874. DOI:10.1111/1752-1688.12949.
16. Toguzova, M.M., Rakhymberdina, M.Y., Kulenova, N.A., Shaimardanov, Z.K., Assylkhanova, Z.A., Apshikur, B. and Beisekenov, N.A. 2022. Analysis of process modeling to support smart agriculture. *Chemical Engineering Transactions*, 94: 871-876. DOI:10.3303/CET2294145.
17. Egorova, E., Semkiv, M., Farinyuk, Y. and Vasiliev, A. 2021. Classification of the Non-Chernozem Zone regions of Russia by agro-climatic and soil indicators. *IOP Conference Series: Earth and Environmental Science*, 852: 012028. DOI:10.1088/1755-1315/852/1/012028.
18. Wang, D., Chen, J., Tang, Z. and Zhang, Y. 2024. Effects of soil physical properties on soil infiltration in forest ecosystems of Southeast China. *Forests*, 15: 1470. DOI:10.3390/f15081470.
19. Tsai, H., Chen, J.H., Huang, W.S., Huang, S.T., Hseu, Z.Y. and You, C.F. 2021. Aeolian additions of podzolic soils on high-altitude mountains. *Geoderma*, 383: 114726. DOI:10.1016/j.geoderma.2020.114726.
20. Kalinitchenko, V.P., Glinushkin, A.P., Sharshak, V.K., Ladan, E.P., Minkina, T.M., Sushkova, S.N. et al. 2021. Intra-soil milling for stable evolution and high productivity of Kastanozem soil. *Processes*, 9: 1302. DOI:10.3390/pr9081302.
21. Sadia, S., Waheed, M., Firdous, S., Arshad, F., Fonge, B.A. and Al-Andal, A. 2024. Ecological analysis of plant community structure and soil effects in subtropical forest ecosystem. *BMC Plant Biology*, 24: 1275. DOI:10.1186/s12870-024-06012-5.
22. Chen, X., Taylor, A.R., Reich, P.B., Hisano, M., Chen, H.Y.H. and Chang, S.X. 2023. Tree diversity increases decadal forest soil carbon and nitrogen accrual. Nature, 618: 94-101. DOI:10.1038/s41586-023-05941-9.
23. Asangaliyev, E.A., Apshikur, B., Lutay, S.S. and Assylkhanova, Z.A. 2024. Spatial analysis and mapping of potential wildFires from Landsat satellite data. *InterCarto. InterGIS*, 30(1): 476-490. DOI:10.35595/2414-9179-2024-1-30-476-490.
24. Brevik, E.C. and Hartemink, A.E. 2021. Soil science and climate change: An overview of recent research and future needs. *Soil Systems*, 5(3): 56. DOI:10.3390/soilsystems5030056.
25. Li, P., Yan, Y., Li, C., Tang, W.G., Xiong, Z.Q. and Tian, Y.H. et al. 2023. Response of rice growth to soil microorganisms and soil properties in different soil types. *Agronomy Journal*, 115: 197-207. DOI:10.1002/agj2.21239.

26. Wei, X., Giles-Hansen, K., Spencer, S.A., Ge, X., Onuchin, A., Li, Q., Burenina, T., Ilintsev, A. and Hou, Y. 2022. Forest harvesting and hydrology in boreal forests. *Forest Ecology and Management*, 522: 120468. DOI:10.1016/j.foreco.2022.120468.
27. Muter, O., Gudra, D., Daumova, G. et al. 2024. Impact of anthropogenic activities on microbial communities in riverbed sediments of East Kazakhstan. *Microorganisms*, 12(2): 246. DOI:10.3390/microorganisms12020246.
28. Shehata, M., Gentine, P., Nelson, N. and Sayde, C. 2022. Characterizing soil water content variability across spatial scales. *Journal of Hydrology*, 612: 128195. DOI:10.1016/j.jhydrol.2022.128195.
29. Abdi, T., Rientjes, T.H.M. and Gieske, A.S.M. 2020. Influence of forest cover and soil properties on runoff generation in a humid tropical catchment. *Science of the Total Environment*, 711: 134671. DOI:10.1016/j.scitotenv.2019.134671.
30. Condon, L., Atchley, A. and Maxwell, R. 2020. Evapotranspiration depletes groundwater under warming over the contiguous United States. *Nature Communications*, 11: 873. DOI:10.1038/s41467-020-14688-0.
31. Mänttäri, M.M., Lindén, L. and Tuhkanen, E-M. 2023. Change in urban forest age structure affects value of ecosystem services. *Frontiers in Sustainable Cities*, 5: 1265610. DOI:10.3389/frsc.2023.1265610.
32. Devi, N.M., Kukarskih, V.V., Galimova, A.A., Mazepa, V.S. and Grigoriev, A. 2020. Climate change evidence in tree growth and stand productivity at the upper treeline ecotone in Polar Ural Mountains. *Forest Ecosystems*, 7(1): 7. DOI:10.1186/s40663-020-0216-9.
33. Bocharnikov, M. 2023. Climate-related gradients on vegetation diversity of the Altai-Sayan Orobiome (Southern Siberia). *Geography, Environment, Sustainability*, 15: 17-31. DOI:10.24057/2071-9388-2022-043.
34. Apshikur, B., Maksimov, V.A., Toleubekyzy, I.T. and Alimkulov, M.M. 2024 (b). Current assessment of atmospheric pollution by industrial enterprises in Ust-Kamenogorsk based on GIS technologies. *InterCarto. InterGIS*, 30(2): 469-481. DOI:10.35595/2414-9179-2024-2-30-469-481.
35. Pérez, J., Brand, C., Alonso, A. et al. 2024. WildFires alter stream ecosystem functioning through effects on leaf litter. *Fire Ecology*, 20: 36. DOI:10.1186/s42408-024-00268-w.
36. Hou, Y., Wei, X., Vore, M., Déry, S.J., Pypker, T. and Giles-Hansen, K. 2022. Cumulative forest disturbances decrease runoff in two boreal forested watersheds. *Journal of Hydrology*, 605: 127362. DOI:10.1016/j.jhydrol.2021.127362.